Journal of Materials and Environmental Sciences
ISSN : 2028-2508
CODEN : JMESCN

J. Mater. Environ. Sci., 2019, Volume 10, Issue 11, Page 1152-1161

http://www.jmaterenvironsci.com

Electro-mechanical, microstructure and corrosion properties of 85Al6063-15CFBP alloy for advance applications

O. S. I. Fayomi [1, 5*], I.G. Akande[2], A.A.A. Atayero[3], A.P.I. Popoola[5], A.A. Ayoola[4]

[1]Department of Mechanical Engineering, Covenant University, P.M.B 1023, Ota, Nigeria.
[2]Department of Mechanical Engineering, University of Ibadan, Ibadan, Oyo state, Nigeria.
[3]Department of Electrical and Information Engineering, Covenant University, Ota, Nigeria.
[4]Department of Chemical Engineering, Covenant University, P.M.B 1023, Ota, Nigeria
[5]Department of Chemical, Metallurgical and Materials Engineering, Tshwane University of Technology, P.M.B. X680, Pretoria, South Africa.

Received 21 Aug 2019,
Revised 13 Oct 2019,
Accepted 14 Oct 2019

Keywords
- ✓ *CFBP,*
- ✓ Corrosion,
- ✓ Metal matrix,
- ✓ Particulates,
- ✓ Resistivity.

ojo.fayomi@covenantuniversity.edu.ng, aigodwin2015@gmail.com;

Phone: +2348036886783

Abstract

In a search for solutions to challenges posed by mechanical and structural degradation of materials in manufacture industry, *Al6063/CFBP composite* was developed via liquid stir casting technique by incorporating *carbonized fish bone powder (CFBP)* into the Aluminium metal matrix in an attempt to provide a material with superior and enduring quality. *0 %, 5 %, 10 % and 15 % of CFBP* was added to the *aluminium metal matrix* during the casting process. The percentage of the *aluminium metal matrix* was of 100, 95, 90, and 85. The gravimetric and potentiodynamic polarization test conducted on the cast *Al6063/CFBP* composite in 0.5 M of hydrochloric acid revealed that the corrosion resisting ability of *Al6063* had been improved. Universal tensile machine and Vickers hardness tester used to conduct the tensile and hardness test respectively affirmed enhanced mechanical properties. More so, the morphological evolution study of *Al6063/CFBP composite* via SEM micrograph unveiled the uniform distribution of CFBP with minimal rifts along the grain boundaries. Electrical characterization of *Al6063/CFBP composite samples* shows that the *CFBP* provided some impressive level of insulation to *Al6063/CFBP composite samples*. This was confirmed by the increase in resistivity of the samples.

1. Introduction

Manufacturing and construction companies have in several years engaged their expertise in the invention of new materials with dynamic and exceptional properties [1, 2]. This engenders the production of Aluminium metal matrix composite which has been employed in numerous industrial applications as a result of their stress cushioning ability. A lot of research has shown that the production of Aluminium metal matrix (AMMCs) composites is economical and affordable, enabling the incorporation of desired properties [3-5]. Generally, AMMCs have been found to exhibit higher deterioration resistance in a contaminated environment when compared to their metallic alloy. This has necessitated the continuous exploration for strengthening of metallic alloys [6, 7]

The selection of strengthening materials usually depends on the desired properties required in the metal matrix composite. The calcium content of carbonized fish bone powder (CFBP) will refine the microstructure of the casting [8] after having prevented ignition during casting [9, 10]. The ignition resisting ability of calcium could be attributed to the evolution of tiny and adhesion of calcium oxide film on the surface of the molten alloy [11]. The coalescence of the initial stage and the final hardness of the composite were improved by the phosphorus and large volume of carbon respectively [12]. The aluminium content of the alloy enhances the castability of the composite by lowering its melting point, without any adverse effect on the strength of the composite, while the minute content of magnesium improves the wettability of the molten state of the stir casting [13].

Although, achievement of a homogeneous dispersion of strengthening particulate is one of the greatest challenges of stir casting process [14]. However, the preference for stir casting over other fabrication techniques is due to its simplicity, mass accommodation ability and low production cost. Several inorganic particles have been used as reinforcing agent of aluminium alloy via stir casting method. TiC is one of the latest with a good show of wettability, thermal stability and even distribution of the particles within the matrix [15-18]. The carbonized husks of rice and maize stalk have also been used for strengthening of Al matrix alloy. These biodegradable materials were found to impact significantly on the performance characteristic Al alloy [19, 20].

More so, the reinforcement ability of orange bark ash particles was investigated, however, a decline in structural properties was the outcome. The decline in structural properties was attributed to the inadequate adhesion ability of the reinforcing particles [21]. This present work utilizes liquid stir casting technique to reinforce Aluminium alloys matrix with carbonized fish bone powder (CFBP). The strengthening effect of CFBP was examined using the gravimetric and potentiodynamic experiment, scanning electron microscope, Vickers hardness and tensile strength measurement.

2. Material and Methods

2.1. Materials in raw form

Al6063 whose composition is shown in Table 1 was used for the fabrication of Al6063-CFBP composite. The fishbone was carbonized using a closed crucible at 400 ^{o}C for 1 hour, pulverized and sieved to 45nano-micron.

Table 1: Percentage weight of Al6063 alloy constituents

Element	S	F	Cu	Mn	Mg	Cr	Ti	Ca	Zr	V	Al
%w	0.157	0.282	0.0025	0.024	0.51	0.023	0.006	0.0011	0.002	0.0035	Bal.

2.2. Production of A6063-CFBPcomposite slurry

The composite slurry was produced from the stir casting set up. The aluminium alloy ingot was melted in the molten chamber which was followed by the addition of CFBP of the desired percentage. The mixture was stirred repeatedly at a regular speed of 500 rmp using mechanical stirrer so as to achieve a homogeneous dispersion of CFBP in the Al6063/CFBP composite slurry [22]. The homogeneous dispersion of Al6063/CFBP is a function of the mechanical stirrer intensity and of the molten temperature [23]. The liquid slurry of Al6063/CFBP was poured in the experimental die set to enable solidification.

2.3. Technical procedures for the preparationA6063/CFBP composite

The preparation of the alloy was carried out in accordance with ASTM B179-06 standard specification for Aluminum Alloys in ingot and molten forms for castings. The furnace used for the casting can withstand the maximum temperature of 1000^{o}C. One kilogram of Al alloy ingot was positioned a graphite crucible and heated to liquid at the temperature 650 ^{o}C. Heating of the ingot was repeated varying the weight concentration of the Al alloy ingot. The CFBP was added to the melted alloy and stirred mechanically in the crucible placed on the furnace at a constant rate to form a vortex. The vortex was poured into a clean die mould made of metal of dimension (100 x 100 x 10) mm between the temperature range of 635 ^{o}C and 650 ^{o}C and allowed to cool and solidify for about 8.5 hours at ambient temperature after which the composite was retrieved from the mould and cut to samples for various experiments.

2.4. Characterization of samples

The microstructural characterizations of the samples were conducted using a Scanning Electron Microscope (SEM) after etching the samples with 0.1 M HCl.The ammeter-voltmeter technique was applied to examine the electrical properties of the samples. The tensile strength and hardness of the samples were studied using UTM-6000 tensile test machine and Vickers hardness techniques respectively. The corrosion resistance capability of the samples was investigated using gravimetric and linear potentiodynamic polarization test.

2.4.1. Electrochemical analysis

The potentiodynamic analysis was conducted using the three electrode system alongside the Auto lab potentiostat in accordance with the work of ref. [24]. Test samples of diameter 20 mm and thickness 5 mm were fastened to the resin and submerged in 0.5 M of HCl at room temperature. The scanning potential ranges from -1.5 V to 1.5 V (OCP) at the rate of 0.005 m/s. The experimental procedure was repeated four times to ensure reproducibility.

The gravimetric experiment was likewise conducted by submerging the sample in 200 ml of 0.5 M of hydrochloric acid at room temperature for 72 (hours) 3 days to determine the weight loss by samples.

2.4.2. Samples Microhardness Characterization

The samples used for the microhardness characterization were of dimension 16 mm x15 mm x10 mm. This was carried out with the use of a testing machine of model HV114. The Vickers testing machine has a ground base of 136 ºC and a diamond pyramid indenter of a square base. The test samples were subjected to a test load 120kgf for 15 seconds in accordance with ASTM: E384 Standard. Three different impressions were conducted with the test load by the indenter on the sample's surface and the impression diagonal were drawn and processed to obtain the Vickers hardness numbers of samples. Using Eqn. 1 [25-27], the Vickers hardness can be calculated numbers.

$$HV = \frac{2P\sin\left(\frac{136}{2}\right)}{a^2} = \frac{1.8544P}{a^2} \quad (1)$$

P is the impression load in kgf, a is the average diagonal of the impression in mm

2.4.3. Tensile strenght test

The tensile strength test was conducted using 600kN capacity servo controlled UTM-6000 tensile test machine. The dog bone shape samples used for this test were drawn to rupture in the computerized UTM-6000 tensile test machine. These samples are of length 100 mm with a cylindrical test region, gauge length of 40 mm and diameter of 1.2 mm. The grip region of the test piece was fastened to the jaws of the UTM-6000 tensile test machine and stretched to rupture by the applied load via the hydraulic drive following ASTM: E0008 standards.

2.4.4. Electrical test of samples

This was carried out with samples of dimension 20 mm x 10 mm x 5 mm. The samples were connected to the voltmeter and ammeter as shown in Figure 1 so as to determine the resistance and current when voltage passes through [28]. The ammeter-voltmeter is an easy, fast and reliable technique for estimating electrical resistance

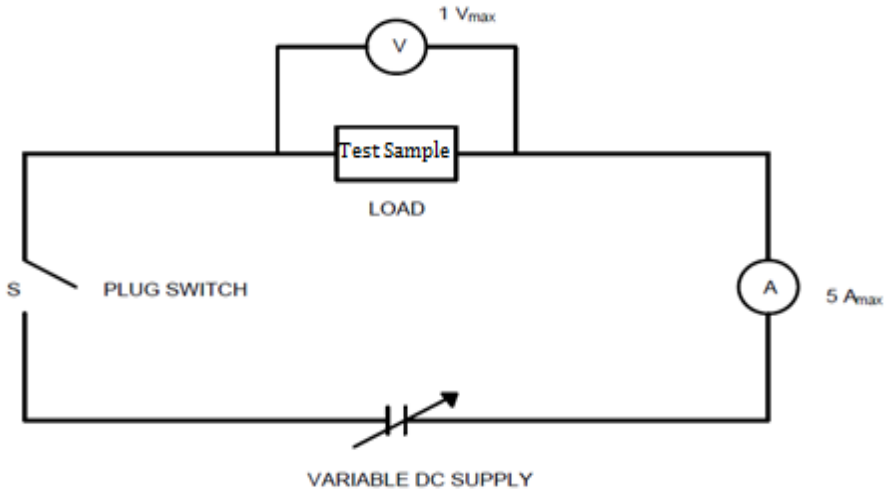

Figure 1: Schematics of the electrical test set up

$$I_R = I - I_V \quad (2)$$

I_R is the current through unknown resistance, I is the current through the ammeter, I_V is the current through voltmeter.

The true value of unknown resistance can be written as:

$$R_x = \frac{V}{I_R} = \frac{V}{I - I_V} \quad (3)$$

The current through the unknown resistance can be written as;

$$I_R = I\left(1 - {}^{V}/_{IR_v}\right) \quad (4)$$

Substituting Eqn.4 into Eqn. 3 give;

$$R_x = \frac{V}{I(1 - {}^{V}/_{IR_v})} \quad (5)$$

V, voltmeter reading,R_v, resistance of voltmeter, Icurrent displayed on the ammeter

The measured resistance value, $R_m = V / I$

i.e. $V / I = R_m$ (6)

Substituting Eqn. 6 into Eqn. 5, gives; Eqn. 7

$$R_x = R_m\left(\frac{1}{1 - {}^{R_m}/_{R_v}}\right) \quad (7)$$

From Eqn. (7), R_x is equal to $R_m$if voltmeter is of infinite resistance. However, if the voltmeter is of extremely large resistance relative to the resistance under measurement,

$R_v >>$ R_m or R_m / R_v is very small.

Therefore,$R_x = R_m[1 + (R_m/R_v)]$ (8)

Thus, the measured value of unknown resistance, R_m is lesser than its true value.

Relative error, $E_x = (R_m - R_x) / R_x$ (9)

3. Results and discussion

3.1. Gravimetric studies and Linear Polarization measurements.

Figure 2 shows the behaviour of the samples after 3 days of immersion in the test solution. From the gravimetric study, it can be seen that the weight loss experienced by the 100%Al6063+0%CFBP sample is higher than other samples. The weight loss was found to reduce as the percentage inclusion of CFBP increases. This reduction in weight loss could be attributed to the inhibitive effect of CFBP on the active site of the Al6063/CFBP composite.

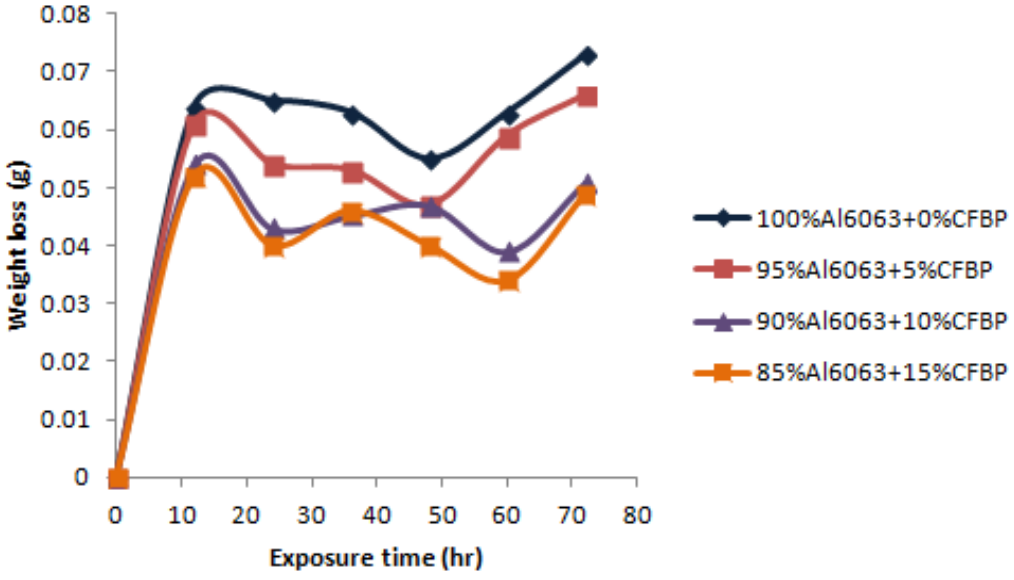

Figure 2: Gravimetric results of Al6063 alloy and Al6063/ CFBP composites

Figure 3 and Table 2 show the Tafel plots and polarization data gotten from the potentiodynamic experiment. The Tafel plots reveal that the Al6063/CFBP samples possess better corrosion resistance. These samples were found to exhibit lower values of corrosion rate (Cr), corrosion current density (jcorr) as shown in Table 2. This shows that the activities of the ions in the active locality of Al6063 alloy were reduced by the CFBP. This is in a good agreement with the gravimetric experiment. The mixed inhibitive characteristic of CFBP was unveiled by the closed value of $E_{corr.}$ This implies that the nano-sized CFBP affected the anodic and cathodic site.

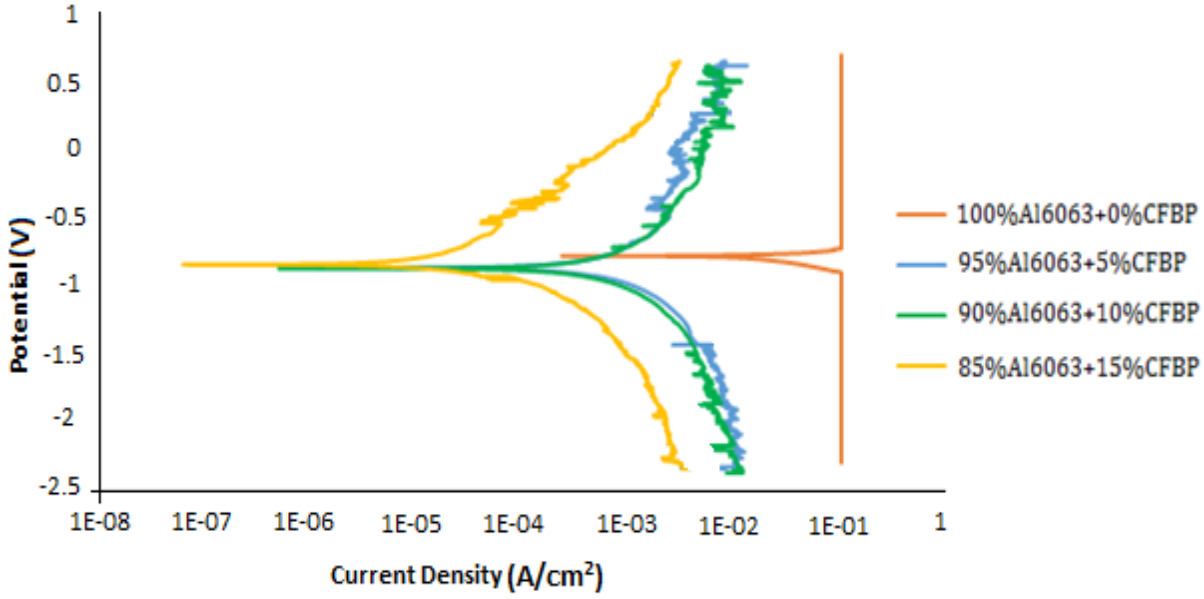

Figure 3: Tafel plots for Al6063alloy and Al6063/CFBP composites.

Table 2: Polarization data for Al6063 and Al6063/CFBP composite

Test Samples	E_{corr} (V)	jcorr (A/cm^2)	Cr (mm/yr)	Rp (Ω)
100%Al6063+0%CFBP	0.8321	6.44E-05	0.7268	37.32
95%Al6063+5%CFBP	0.8573	5.12E-05	0.6241	146.90
90%Al6063+10%CFBP	0.8515	4.93E-05	0.5502	185.43
85%Al6063+15%CFBP	0.8410	4.32E-05	0.4828	206.72

3.2. Microhardness properties of Al6063 alloy and Al6063/CFBP composite

Figure 4 shows the Vickers microhardness properties of the test samples. Microhardness was found to increase as the percentage weight of CFBP increases. 85%Al6063+15%CFBP sample exhibit the highest hardness value of 67.48 kgf/mm^2. Generally, all the samples with CFBP inclusion registered an increase in microhardness. The notable increase in microhardness could be linked with the structural modification by CFBP in the matrix of Al6063 alloy. The effect CFBP on the microhardness was further examined by estimating the change in the microhardness with respect to the level to level percentage weight inclusion of CFBP as shown in Figure 5. The maximum increase in the value of microhardness was obtained between 10 and 15 CFBP % inclusion. This might be attributed to the high volume of carbon around the test area.

3.3. Tensile strenght examination of Al6063 alloy and Al6063/CFBP composite sample

The result of the tensile strength test carried out on the samples is shown in Figure 6.The tensile raises on the addition of 5% CFBP from 138.40 N/mm^2 to 146.32 N/mm^2.Generally, the tensile strength increases as the percentage weight of CFBP increases. Although, a little increment in tensile strength was observed on the inclusion of 10 % CFBP, however, a notable increase was observed with the 15 % addition of CFBP affirming its reinforcement ability.

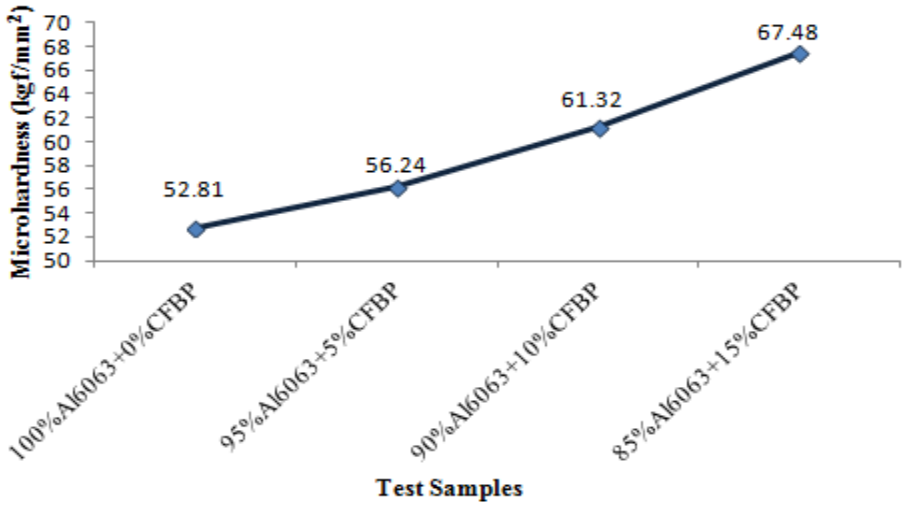

Figure 4: Vickers microhardness of Al6063 alloy and Al6063/CFPB composite samples

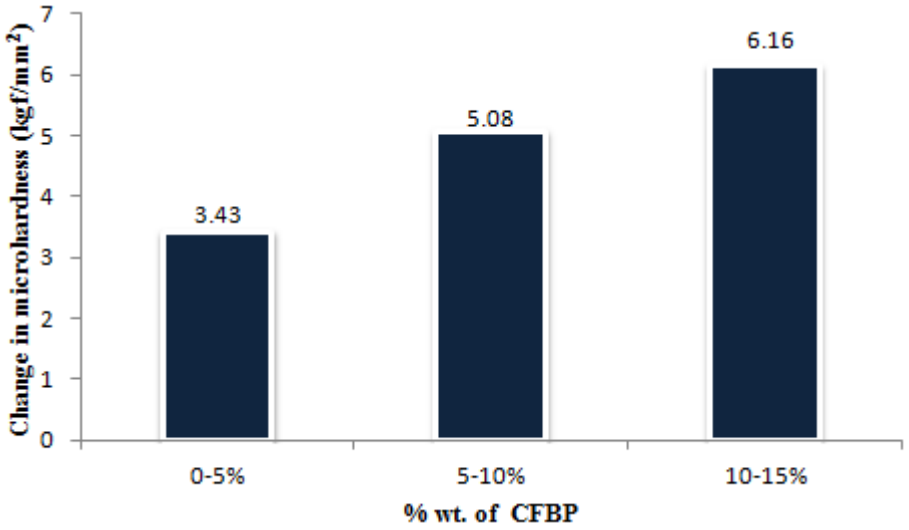

Figure 5: Comparison of change in microhardness on level to level inclusion of CFBP

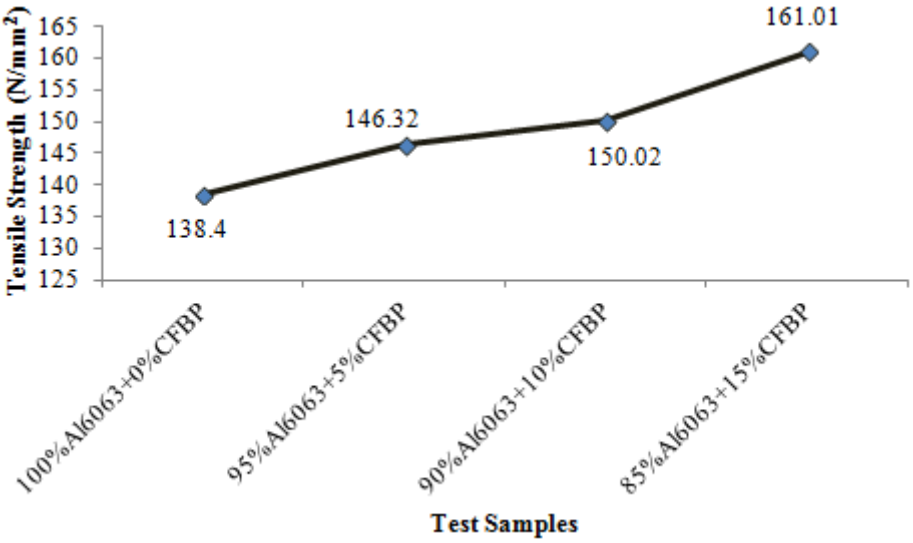

Figure 6: Tensile Strenght of Al6063 alloy and Al6063/CFBP composite samples

CFBP effect on the tensile strength was further examined by estimating the change in the tensile strength with respect to the level to level percentage weight inclusion of CFBP as shown in Figure 7. The maximum increase in the value of tensile strength was obtained between 10 and 15CFBP % inclusion while the minimum is between 5 and 10CFBP % inclusion. This irregularity could be as a result of the change in the ductility of the composite in the micro level site close to the CFBP [29].

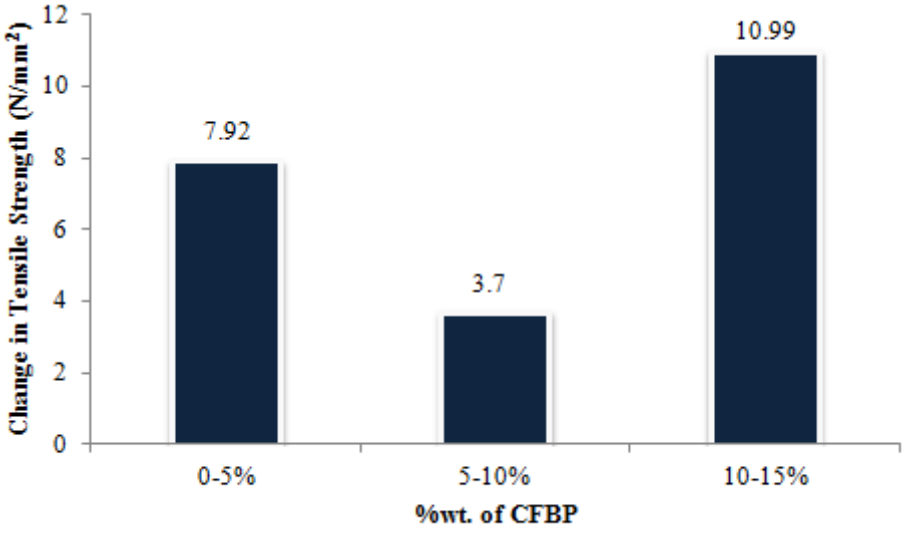

Figure 7: Comparison of change in tensile strenght on level to level inclusion of CFBP

3.4. Effect of CFBP on the Electrical property of the samples

Figure 8 shows the effect of CFBP on the electrical resistivity of Al6063 alloy after passing a maximum current of 2.0 A through the samples. The electrical resistivity of the alloy increases as the per cent weight of CFBP in the matrix increases. 85%Al6063+15%CFBP sample exhibit the maximum electrical resistivity value of 2.28 Ωmm. This is an indication that CFBP possesses inherent electrical insulating characteristics.

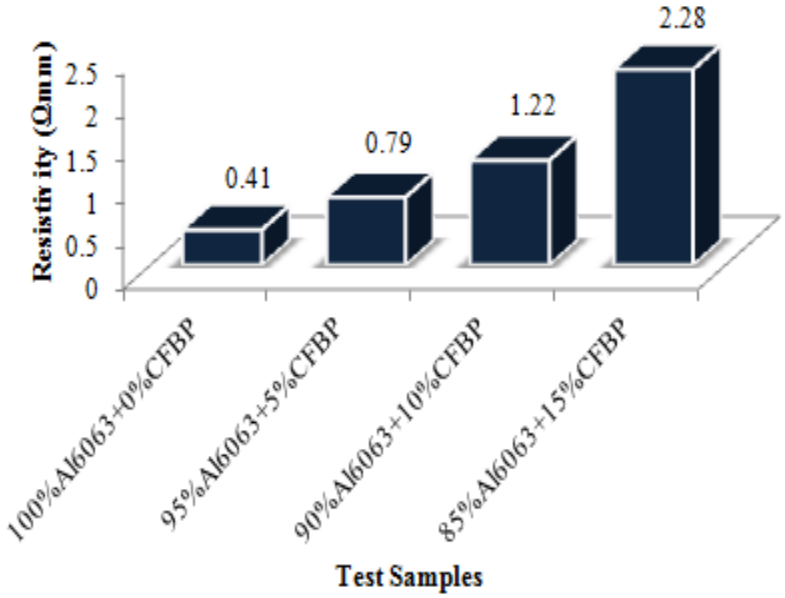

Figure 8: Electrical resistivity of Al6063 and Al6063/CFBP composite samples

More so, Figure 9 presents the effect of CFBP on electrical conductivity. Expectedly, conductivity reduces as the percentage of CFBP increases. This behaviour further confirmed the insulating attribute of CFBP in the alloy matrix.

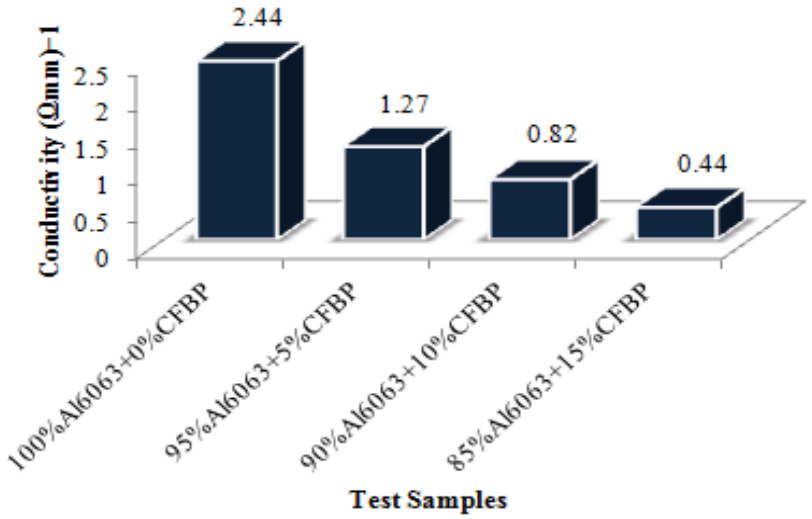

Figure 9: Electrical conductivity of Al6063 alloy and Al6063/CFBP composite samples

3.6. Morphology and Structure of Al6063 alloy and Al6063/CFBP Composite samples

Figure 10a-d shows the SEM images of all the test samples. Figure 10b-d unveiled homogenously dispersion of CFBP in Al6063/CFBP composite matrix with reduced porosity. Plenty of pores were observed in the SEM micrograph in Figure 10a. The presence of plenty of pores in Figure 10a could be attributed to the none inclusion of CFPB in the matrix of the alloy, leading to large entrapment of gases during casting [30, 31]. In Figure 10d, the recrystallization level was low compared to Figure 10b and Figure. 10c due to the developed barriers as a result of the higher percentage of CFPB [32]. Figure 10a exhibits active re-crystallization in Al6063 via the creation of new grains in the previous grain boundaries.

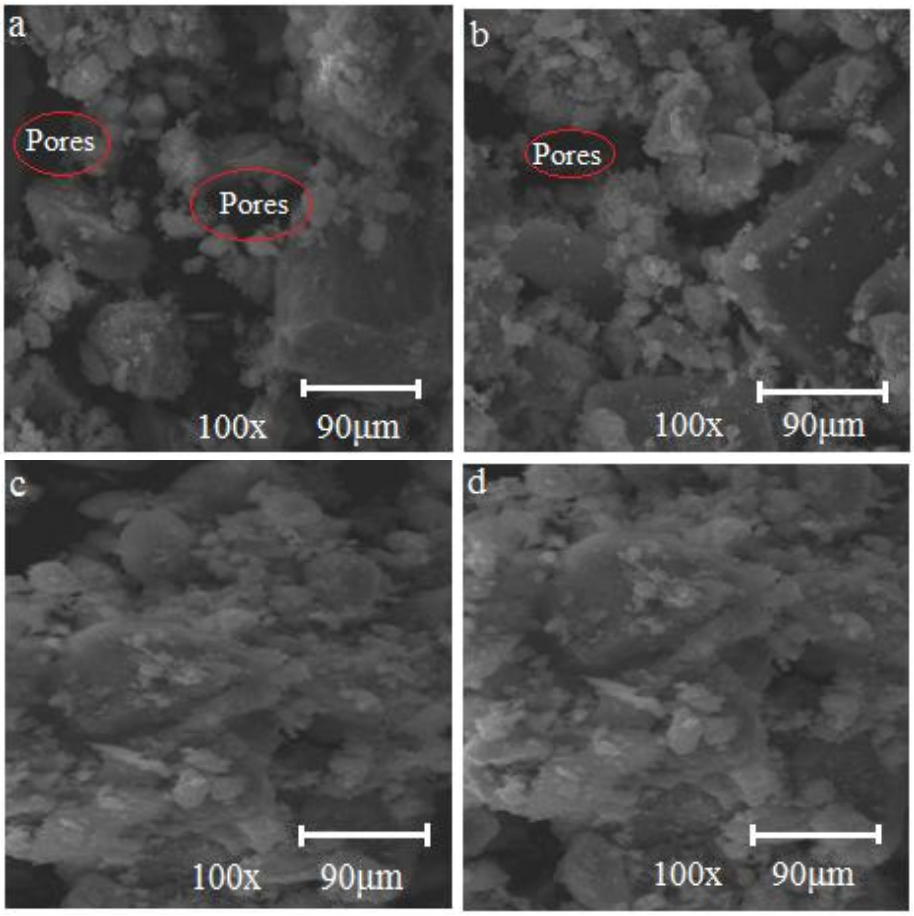

Figure 10: SEM micrograph of (a) 85%Al6063+15%CFBP (b) 85%Al6063+15%CFBP (c) 85%Al6063+15%CFBP (d) 85%Al6063+15%CFBP Samples

Conclusion

The CFPB addition into Al6063 alloy resulted in improved performance characteristics. The electrochemical experiments confirmed the corrosion protective effect of CFPB. The tensile strength and microhardness of the alloy improved significantly as the percentage weight of CFPB increases. The morphological analysis with SEM unveiled the homogeneous dispersion of the reinforcing CFPB along the grain boundaries of Al6063/CFPB composite. The SEM micrographs also revealed reduced porosity on the inclusion of CFPB in the matrix of Al6063 alloy. These improvements in properties show that reinforced material is suitable for advance application.

References

1. I. Balasubramanian, R. Maheswaran R, Effect of inclusion of SiC particulates on the mechanical resistance behaviour of stir-cast AA6063/SiC composites. *Materials & Design*. 65 (2015) 11-20
2. O.S.I, Fayomi, O.O. Joseph, I.G. Akande, C.K. Ohiri, K.O. Enechi, N.E. Udoye, Effect of CCBP doping on the multifunctional Al-0.5 Mg-15CCBP superalloy using liquid metallurgy process for advanced application. *Journal of Alloys and Compounds*. 783 (2019) 246-255.
3. M.F. Ibrahim, E. Samuel , A.M. Samuel, A.M. Al-Ahmari, F.H. Samuel, Metallurgical parameters controlling the microstructure and hardness of Al–Si–Cu–Mg base alloys. *Materials & Design*. 32 (2011) 2130-2142.
4. O.S.I. Fayomi, I.G. Akande, A.P.I. Popoola, Corrosion Protection Effect of Chitosan on the Performance Characteristics of A6063 Alloy. Journal of Bio-and Tribo-Corrosion. 4 (2018). 73-7
5. M. Dave, K. Kothari, Composite material-aluminium silicon alloy: a review. Paripex-Indian *Journal of Research*. 2 (2013) 148-150.
6. A.P. Subrahmanyam, J. Madhukiran, G. Naresh, S. Madhusudhan, Fabrication and Characterization of Al356. 2, Rice Husk Ash and Fly Ash Reinforced Hybrid Metal Matrix Composite. *International Journal of Advanced Science and Technology*. 94 (2016) 49-56.
7. B.A. Kumar, N. Murugan, Metallurgical and mechanical characterization of stir cast AA6061-T6–AlNp composite. *Materials & Design.* 40 (2012) 52-58.
8. P. Li, B. Tang, E.G. Kandalova, Microstructure and properties of AZ91D alloy with Ca additions. *Materials Letters.* 59 (2005) 671-67.
9. A. Kitahara, S. Akiyama, H. Ueno, M. Sakamoto, H. Hirai, Development of noncombustible magnesium alloys. *Materia Japan(Japan)*. 39 (2000) 72-74.
10. J.P. Park, M.G. Kim, U.S. Yoon, W.J. Kim, Microstructures and mechanical properties of Mg–Al–Zn–Ca alloys fabricated by high frequency electromagnetic casting method. *Journal of materials science.* 44 (2009) 47-54
11. S. Guo, Q. Le, Z. Zhao, Z. Wang, J. Cui, Microstructural refinement of DC cast AZ80 Mg billets by low frequency electromagnetic vibration. *Materials Science and Engineering.* 404 (2005) 323-329.
12. N. Rugayah, H. Nuraini, Chicken bone charcoal for defluoridation of groundwater in Indonesia. *International Journal of Poultry Science.* 13 (2014) 591-596.
13. B. Suárez-Peña, J. Asensio-Lozano, J.I. Verdeja-Gonzalez, J.A. Pero-SanzElorz, Microstructural effects of phosphorus on pressure die cast Al-12Si components. *Revista de metalurgia*. 43 (2007) 352-358.
14. M.O. Shabani, A. Mazahery, The synthesis of the particulates Al matrix composites by the compocasting method. *Ceramics International.* 39 (2013) 51-58.
15. S.B. Boppana, K. Chennakeshavalu, Preparation of Al-5Ti Master Alloys for the In-Situ Processing of Al-TiC Metal Matrix Composites. *Journal of Minerals and Materials Characterization and Engineering*.8 (2009) 563-568.
16. A. Kumar , M.M. Mahapatra , P.K. Jha , Fabrication and characterizations of mechanical properties of Al-4.5% Cu/10TiC composite by in-situ method. *Journal of Minerals and Materials Characterization and Engineering*. 11 (2012) 1075-1080.
17. M. Singla, D.D. Dwivedi, L. Singh, V. Chawla, Development of aluminium based silicon carbide particulate metal matrix composite. *Journal of Minerals and Materials Characterization and Engineering*. 8 (2009) 455-467.
18. A. Albiter , C.A. Leon, R.A. Drew ,E. Bedolla , Microstructure and heat-treatment response of Al-2024/TiC composites. *Materials Science and Engineering.* 289 (2000)109-115.
19. S.B. Hassan, V.S. Aigbodion, The study of the microstructure and interfacial reaction of Al–Cu–Mg/bagasse ash particulate composite. *Journal of Alloys and Compounds.* 491 (2010) 571-574.
20. A.A. Ahamed, R. Ahmed, M.B. Hossain, M. Billah. Fabrication and characterization of aluminium rice husk ash composite prepared by stir casting method. *Rajshahi University Journal of Science and Technology*. 44 (2016) 9-18.

21. J.E. Oghenevweta , V.S. Aigbodion, G.B. Nyior , F. Asuke . Mechanical properties and microstructural analysis of Al–Si–Mg/carbonized maize stalk waste particulate composites. *Journal of King Saud University-Engineering Sciences.* 28 (2016) 222-229.
22. M. Kok, Production and mechanical properties of Al_2O_3 particle-reinforced 2024 aluminium alloy composites. *Journal of Materials Processing Technology*. 161 (2005) 381
23. M. Ramachandra, K. Radhakrishna, Sliding wear, slurry erosive wear, and corrosive wear of aluminium/SiC composite. *Material science-wroclaw.* 24 (2006) 333- 349.
24. O.S.I. Fayomi, I.G. Akande, O.O. Oluwole, D. Daramola, Effect of water-soluble chitosan on the electrochemical corrosion behaviour of mild steel. *Chemical Data Collections.* 17 (2018) 321-326.
25. O. Uzun, T. Karaaslan, M. Gogebakan, M. Keskin, Hardness and microstructural characteristics of rapidly solidified Al–8–16 wt.% Si alloys. *Journal of Alloys and Compounds*. 376 (2004)149-157.
26. Krishna, M. Karthik, Evaluation of Hardness Strength of Aluminium Alloy (AA6061) Reinforced With Silicon Carbide. International Journal on Recent Technologies in Mechanical and Electrical Engineering. 1 (2014) 14-18.
27. I.L. Denry, J.A. Holloway, Elastic constants, Vickers hardness, and fracture toughness of fluorrichterite-based glass–ceramics. *Dental Materials.* 20 (2004), 213-219.
28. K.F. Ayarkwa, S.W. Williams, J. Ding, Assessing the effect of TIG alternating current time cycle on aluminium wire arc additive manufacture. *Additive Manufacturing.* 18 (2017) 186-193.
29. I. Balasubramanian, R. Maheswaran, Effect of inclusion of SiC particulates on the mechanical resistance behaviour of stir-cast AA6063/SiC composites. *Materials & Design* (1980-2015) 65 (2015) 511-520.
30. A. Alizadeh, E. Taheri-Nassaj, M. Hajizamani. Hot extrusion process effect on mechanical behavior of stir cast Al based composites reinforced with mechanically milled B4C nanoparticles. *Journal of Materials Science & Technology*. 27 (2011) 1113-1119.
31. M.K. Akbari, O. Mirzaee, H.R. Baharvandi, Fabrication and study on mechanical properties and fracture behavior of nanometric Al_2O_3 particle-reinforced A356 composites focusing on the parameters of vortex method. *Materials & Design*. 46 (2013) 199-205.
32. H.R. Ezatpour ,S.A. Sajjadi , M.H Sabzevar ,Y. Huang . Investigation of microstructure and mechanical properties of Al6061-nanocomposite fabricated by stir casting. *Materials & Design*. 55 (2014) 921-928.

(2019); http://www.jmaterenvironsci.com